nature photonics

Article

https://doi.org/10.1038/s41566-025-01747-5

Broadband optical fibre with an attenuation lower than 0.1 decibel per kilometre

Received: 4 April 2025

Accepted: 22 July 2025

Published online: 01 September 2025

Check for updates

Marco Petrovich[1,3], Eric Numkam Fokoua[1,3], Yong Chen[1], Hesham Sakr[1], Abubakar Isa Adamu[1], Rosdi Hassan[1], Dong Wu[1], Ron Fatobene Ando[1], Athanasios Papadimopoulos[1], Seyed Reza Sandoghchi[1], Gregory Jasion[2] & Francesco Poletti[1,2]

A critical component of optical communications is the availability of a suitable waveguide technology for the transport of electromagnetic waves with low loss over a broad spectral range. In the past four decades, despite extensive research, the attenuation and spectral bandwidth of silica-based optical fibres have remained relatively unchanged, with state-of-the-art fibres offering values of 0.14 dB km^{-1} and 26 THz below 0.2 dB km^{-1}, respectively. Here we report a microstructured optical waveguide with unprecedented transmission bandwidth and attenuation, with a measured loss of 0.091 dB km^{-1} at 1,550 nm that remains below 0.2 dB km^{-1} over a window of 66 THz. Instead of a traditional solid glass core, this innovative optical fibre features a core of air surrounded by a meticulously engineered glass microstructure to guide light. This approach not only reduces attenuation and other signal degradation phenomena, but it also increases transmission speeds by 45%. Furthermore, the approach theoretically supports further loss reductions and operation at wavelengths where broader bandwidth amplifiers exist, potentially heralding a new era in long-distance communications as well as remote delivery of laser beams.

The quest for long-distance communication has driven human creativity for centuries, from the use of fire beacons at night in the Old and Middle Ages, to the mechanical optical telegraphs of the Napoleonic era, up to the groundbreaking electric telegraphs of the 1850s. The transmission of the first Morse-coded message across the Atlantic via a sub-sea telegraph cable in 1858 was a monumental achievement that shrank geographical divides and revolutionized communication[1]. The realization in the early twentieth century that modulated radio waves could be reflected by the ionosphere further enhanced communication capabilities, thus enabling long-distance communications even in the absence of a direct connection and of a line of sight[2]. However, the inherent noisiness, unreliability and limited bandwidth of radio wave communication prompted the development of higher-quality cables that could transmit multiple voice calls simultaneously. Heaviside's coaxial cable[3], with suitably developed conductive and insulating materials, became the technology that underpinned long-distance transmissions for decades. The transition from coaxial cables to optical fibres marked another notable milestone in communication technology. The pioneering work of Kao and Hockham in the 1960s identified the potential of using purified glass for transmitting modulated optical signals (hence information) to kilometre-scale distances[4], leading to the development of low-loss optical fibres by Corning in the 1970s[5]. This innovation ushered in the era of digital optical communications, which for the last half a century has formed the backbone of global telecommunication networks and enabled the internet revolution[6]. Is a further step ahead possible?

All these breakthroughs were driven by the primary objective to transmit more information, as either more simultaneous messages and voice calls in the analogue electrical era or more bits per second in the digital age. A second, non-negligible goal has always been the

[1]Microsoft Azure Fiber, Romsey, UK. [2]Optoelectronics Research Centre, University of Southampton, Southampton, UK. [3]These authors contributed equally: Marco Petrovich, Eric Numkam Fokoua. e-mail: fp@soton.ac.uk

reduction of the attenuation (or 'loss') of the transmission medium, to increase the distance that a signal could reach before needing regeneration or amplification. Shannon's mathematical theory of information linked the two goals: lower attenuation required less amplification; the resulting improvement in the signal-to-noise ratio enabled the system to increase its maximum throughput of information[7].

Upshifting the frequency of the modulated signal carrier from tens of MHz used in the long-distance electrical coaxial cables to hundreds of THz used in optical communications enabled an increase in information throughput of more than a million times. Simultaneously, optical fibres also presented an ultralow level of attenuation of around 0.15 dB km^{-1}, which remained approximately constant over a bandwidth of ~10 THz where optical amplification from erbium-doped fibre amplifiers was available. This was a substantial improvement over coaxial cables, where attenuation was frequency dependent (as $\sqrt{f}$) and reached much higher values than optical fibres at the top frequencies (for example, ~4.5 dB km^{-1} at 30 MHz in the transatlantic TAT-6 cable[8]).

Despite unrelented progress in the field of optical communications since 1970, the minimum attenuation of silica glass fibres has remained approximately unchanged for more than four decades: from 0.154 dB km^{-1} in 1985[9] to 0.1396 dB km^{-1} in 2024[10]. The seemingly insurmountable attenuation limit of ~0.14 dB km^{-1} for information-carrying waveguides has so far hindered further breakthroughs in communication systems. It has also forced technology to converge to this relatively narrow frequency range of only 5% of the carrier frequency (10 THz at around 192 THz).

Having failed in many decades to identify and synthetize a more transparent glass than silica, a potential route to further lower the propagation loss of a long-distance communication waveguide is to avoid the scattering and absorptions introduced by the glass and which cause loss of signal power in telecoms fibres. This can be achieved by transmitting electromagnetic radiation in a hollow region rather than through a solid glass core. Theoretical foundations[11], early loss estimates[12] and first experiments[13,14] for cylindrical, metal, hollow waveguides pre-dated the development of ultra-pure glass fibres. Experimental works from Bell Labs in the mid-twentieth century with dielectric-coated metallic hollow pipes (WT4) reached losses as low as 0.5 dB km^{-1} at frequencies of 70 GHz and impressive capacities of 476,000 voice channels[15]. The technology was however discarded in the mid-1970s for installation complexities and techno-economic reasons.

New research in the late 1990s and 2000s investigated the potential for achieving ultralow loss at visible/near-infrared frequencies by transmitting light through hair-thin flexible hollow core fibres (HCFs). These glass-based waveguides could transmit light in an air core, thanks to a periodic 'holey' cladding around it that created an out-of-plane photonic bandgap[16–19]. While such research produced an outstanding new tool for scientific investigations, it failed to attain fibres with attenuation below 1 dB km^{-1} and with adequate modal purity for long-distance communication. It is only with the advent of a second generation of HCFs, guiding light through antiresonances and inhibited coupling effects in sub-wavelength-thick, core-surrounding membranes[20], and with the introduction of nested tube designs[21,22], that the prospect of achieving sub-0.14 dB km^{-1} losses became viable[22]. Over the last 6 years, through improved designs and engineering, loss in these nested or double nested antiresonant nodeless hollow core fibres (NANFs/DNANFs) has decreased by an order of magnitude, reaching near parity with the fundamental attenuation of silica glass telecoms fibres at 1,550 nm (ref. 23), and lower values at both shorter[24–26] and longer[27] wavelengths.

In this work, we showcase the latest advancements in hollow core DNANF technology and present the first optical waveguide that surpasses conventional optical fibres in both loss and bandwidth simultaneously. With a measured loss of under 0.1 dB km^{-1} across an 18 THz bandwidth, this breakthrough result paves the way for a potential revolution in optical communications, enabling unprecedented data transmission capacities, more energy-efficient optical networks and longer unamplified spans.

Fibre fabrication and characterization

Optimizing the loss of hollow core DNANFs requires in-depth understanding and accurate models of all its three primary components: leakage loss (LL), surface scattering loss (SSL) and microbend loss (μBL). Each mechanism has a different dependence on the geometrical features of the fibre's cross section and on the operating wavelength[28]. SSL and μBL models require statistical characterization of the surface roughness of the microstructure's glass membranes and of the micro perturbations external to the fibre, respectively, that cannot be acquired with adequate accuracy at all spatial frequencies. To circumvent the problem, we fit the free parameters in well-established SSL and μBL models[28] so that good match between measured and simulated loss is achieved simultaneously for a statistically significant number of different DNANFs fabricated according to our processes[29]. Figure 1 shows the excellent overall agreement between the measured loss of a DNANF, randomly chosen among the 15 different fibres that we used to fit our models, and our modelling prediction. As can be seen, the three loss mechanisms have notably different spectral behaviours, but, when added together, they reproduce accurately the measured fibre loss, not only in the fundamental antiresonant window (~1,300 nm to >1700 nm) where SSL provides the largest contribution, but also in the second window (~750–840 nm) where μBL dominates.

We then used this calibrated loss model to optimize the fibre geometry. To produce the widest possible low-loss bandwidth, we targeted a fibre in which the (widest) first antiresonance window is centred at 1,550 nm. Besides, we also aimed to achieve sufficiently high modal purity to yield an intermodal interference (IMI) of better than −60 dB km^{-1}, adequate to maintain a negligibly low penalty in long haul distance transmissions[30,31]. Modelling predictions indicate that for core sizes between 25 μm and 36 μm, total losses below 0.1 dB km^{-1} are possible, with the dominant contribution shifting from SSL to μBL as the core enlarges. In this work, we settled on a core diameter of ~29 μm, theoretically capable of achieving a loss as low as 0.07 dB km^{-1}.

Driven by modelling guidance, we fabricated a first fibre (HCF1) with a core diameter of 28.8 ± 0.5 μm and average diameters of the nested tubes of 31.0 ± 1.5 μm (large tubes), 28.8 ± 2 μm (middle) and 10.0 ± 3 μm (small). The membrane thicknesses for all tubes were around 500 nm, tailored to centre the fundamental antiresonance window at 1,550 nm, and the fibre length is 4.12 km (ref. 29). We used three different methods to characterize its loss. As predicted by modelling, this was measured to be lower than that of glass-core fibres. However, owing to the short fibre length available and its record low level of loss, despite extreme care in performing the measurements, three different techniques yielded rather different loss values. At 1,550 nm, two independent cutbacks averaged a loss of 0.055 dB km^{-1} and 0.065 dB km^{-1}; through an insertion loss measurement, we obtained 0.09 ± 0.01 dB km^{-1}, while with an optical time-domain reflectometer (OTDR), we measured 0.11 ± 0.01 dB km^{-1} (ref. 29). This clearly indicates that considerably longer fibres are needed for accurate measurements.

After our disclosure[29], another team reported fabrication of a DNANF variant that achieved similar loss values, in the range of 0.1–0.13 dB km^{-1} and very high suppression of high-order modes. The fibre had four rather than five sets of double nested tubes, semicircular outer tubes and a core size in the range of 29–31 μm (ref. 32). Its fabricated lengths were similar to our HCF1, with five bands between 2.3 km and 4.2 km. The thicker membranes (~1.1 μm versus ~0.5 μm of our work) make fabrication easier at the expense of a considerably narrower bandwidth. While such a fibre concept might be a good candidate for data transmission in the C or C + L telecommunication bands, it is intrinsically unable to support the ultrawide band operation that we seek in this work.

https://doi.org/10.1038/s41566-025-01747-5

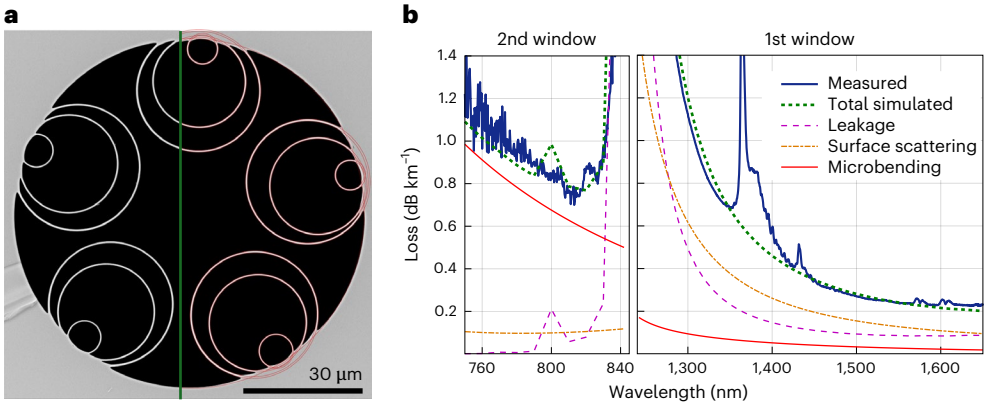

Fig. 1 | Modelling validation. a, Scanning electron microscope (SEM) image of the cross section of one of the DNANFs used to calibrate our loss model. In red, the automatic edge extraction of the tubular resonators used to inform simulations. **b**, Measured loss of the same fibre and simulation of its leakage, surface scattering and microbend loss. The total simulated loss shows good agreement with the measurement in both the first (right) and second (left) antiresonant windows, despite being dominated by different mechanisms.

We then worked on upscaling the fabricated length of our first-window DNANF concept and produced HCF2. The fibre cross section is shown in Fig. 2a. Its geometry closely resembles that of HCF1, with a core diameter varying between 29.1 µm and 29.6 µm across the full length. The diameters of the nested tubes vary azimuthally and longitudinally between 30.4 µm and 31.7 µm (large), 22.7 µm and 24.8 µm (middle) and 7.0 µm and 8.4 µm (small). The fibre length is 15 km, which allows for substantially improved accuracy in its loss measurement. Figure 2b shows OTDR measurements at 1,310 nm and 1,550 nm, indicating a uniform loss with a slope of 0.123 dB km^{-1} and 0.095 dB km^{-1}, respectively. To validate these measurements, we performed four separate cutbacks on the fibre, using two different methods. The green band in Fig. 2c shows the 95% confidence level of these four measurements around the mean loss curve, shown in dark blue (Methods). We also performed an additional cutback using an optical spectrum analyser (OSA) capable of measuring wavelengths in the 1,650–1,900 nm range and of capturing the full spectral transmission bandwidth of the fibre (light blue curve in Fig. 2c). As can be seen in the zoomed-in plots of Fig. 2d, the average loss is 0.128 dB km^{-1} and 0.091 dB km^{-1} at 1,310 nm and 1,550 nm, respectively. This is in good agreement with the OTDR measurements, which fall within the confidence level of the cutback measurements. The loss is below 0.1 dB km^{-1} between 1,481 nm and 1,625 nm. Remarkably, a lower loss than the current 0.14 dB km^{-1} record of solid-core fibres is also achieved in the O band, between 1,292 nm and 1,347 nm.

The loss curve in Fig. 2c shows signs of absorptions from gaseous species present in the core of the fibre. Comparison with data from the HITRAN database[33] allows one to identify absorptions from water vapour, carbon dioxide and some nitrogen oxides, likely to arise from residual atmospheric gases in the fibre's preform, as well as hydrogen chloride originating from the use of chlorinated glass tubes to make the fibre. None of these absorptions is a fundamental property of the fibre, and improved fabrication processes are expected to lead to a reduction or elimination of these absorption features. For example, use of glass with no chlorine would straightforwardly eliminate the HCl lines and open an 18.5 THz absorption-free window between 1,620 nm and 1,800 nm, where the low-loss region could be tuned (see later). CO_2, water vapour and NO_x gases are unintentionally added to the hollow regions of the fibre during the fabrication and could be substantially reduced through process improvements. Besides, all these absorption lines have a narrow linewidth (of the order of a few picometres) and occur at known frequencies, which makes it possible to foresee the development of transmission strategies to compensate for their presence.

Besides the loss, we also measured the IMI and the polarization properties of the fibre around 1,550 nm. IMI was measured to be as low as −70 dB km^{-1}, which according to previous studies would add no measurable penalty for any long-distance data transmission[30,31]. The fibre's polarization-dependent loss and polarization mode dispersion coefficients are 0.013 dB √km^{-1} and 0.1 ps √km^{-1}, respectively, not too dissimilar from those of standard telecoms fibres.

Figure 3a shows how the mean loss of HCF2 compares with that of the pure silica core fibre (PSCF) with the lowest loss reported so far (0.1397 dB km^{-1} at 1,550 nm; Sato et al.[10]). For visual comparison, we also show the loss curve of the record low-loss fibre in 2002 from Nagayama et al.[34]. In this fibre, the loss was measured across a broad wavelength range (1,250–1,750 nm), which helps comparing the fundamental spectral bandwidth of silica versus that of HCF2. The difference between Nagayama's and Sato's fibres also shows the progress of solid core research fibres in the last 23 years. As can be seen, neglecting gas absorptions, HCF2 has a fundamental attenuation of less than 0.14 dB km^{-1} over a 424 nm bandwidth centred at 1,504 nm (corresponding to 54.3 THz), and of less than 0.1 dB km^{-1} in a 144 nm (17.9 THz) spectral region around 1,553 nm.

Figure 3b shows the modelled dispersion of HCF2, with 2.1 ps nm^{-1} km^{-1}, 3.2 ps nm^{-1} km^{-1} and 3.7 ps nm^{-1} km^{-1} at 1,310 nm, 1,550 nm and 1,700 nm, respectively, and compares it with that of the record low-loss PSCF[10]. Not only has HCF2 lower loss and broader bandwidth, but also it presents a 7 times reduction in chromatic dispersion (3.2 ps nm^{-1} km^{-1} versus 21.8 ps nm^{-1} km^{-1} at 1,550 nm) and a 17 times reduction in dispersion slope. For coherent transmissions, this enables simplifications in the transceiver's digital signal processing complexity and energy consumption; for intensity modulation-direct detection used in shorter reach transmission, it enables longer transmission lengths without dispersion compensation[35].

Further improvements and discussion

After discussing the performances of HCF2, we will now extrapolate the optical properties that these types of HCF could ultimately offer with further engineering work. Figure 4a shows once again the loss of state-of-the-art PSCF telecoms fibres. The minimum loss of ~0.14 dB km^{-1} is achieved in a spectrally narrow region of around 20 nm around 1,550 nm. Approximately 10 THz can be guided in the C and L telecommunication bands with a loss below 0.145 dB km^{-1}, and 26 THz can be transmitted with a loss below 0.2 dB km^{-1} (ref. 9). The red curves show the fundamental loss (that is, with gas absorption omitted) of the fabricated HCF2 (dashed) and of an ideal DNANF having the same nominal geometry, cladding and core diameters, with a

https://doi.org/10.1038/s41566-025-01747-5

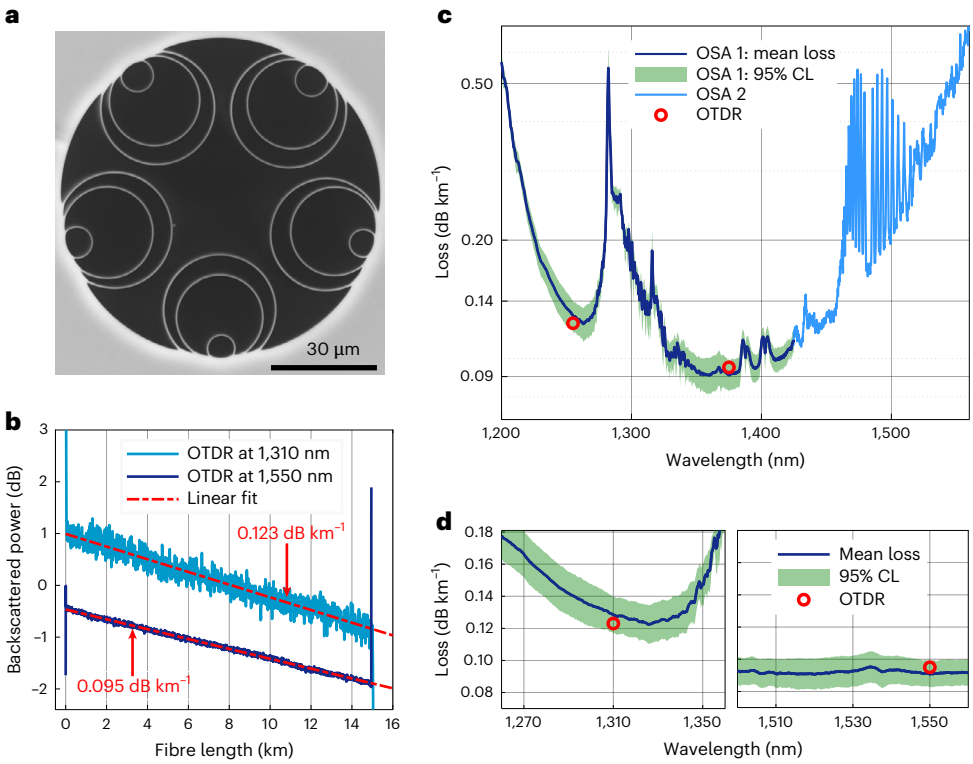

Fig. 2 | Characterization of the fabricated fibre. a, SEM of the fabricated HCF2. **b**, Bi-directional OTDR traces at 1,310 nm and 1,550 nm. **c**, Mean loss and 95% confidence level (CL) of four separate cutbacks (1,200–1,650 nm) compared with OTDR results and a fifth cutback to show the spectral loss in the 1,650–1,950 nm range. **d**, Cutback loss details in the 1,270–1,350 nm and 1,500–1,560 nm bands.

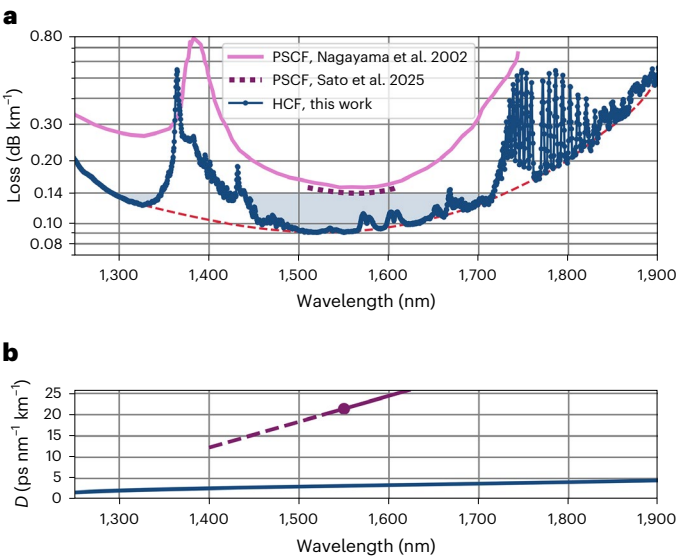

Fig. 3 | Loss and chromatic dispersion comparison with state-of-the-art telecoms fibres. a, Loss of the DNANF in this work, compared with that of the record low-loss PSCFs from 2002 (Nagayama et al.[34]) and 2025 (Sato et al.[10]). **b**, Simulated dispersion of the DNANF and measured dispersion of the PSCF from Sato et al.

perfect transverse and longitudinal uniformity. Its loss at 1,550 nm is predicted to be 0.07 dB km^{-1} and the bandwidth where this remains below 0.2 dB km^{-1}, 0.14 dB km^{-1} and 0.1 dB km^{-1} is 92 THz, 78 THz and 54 THz, respectively. The figure also shows five other designs, where we have rigidly scaled all the membrane thicknesses by a common factor to shift their antiresonance window at wavelengths around 850 nm, 1,060 nm, 1,310 nm, 1,700 nm and 2,000 nm. In each case, the core size has been optimized so that the total loss contribution from LL, SSL and µBL is minimized (Methods). As can be seen, by using one of these HCF designs, losses below 0.2 dB km^{-1}, compatible with long-distance communications, become possible from 700 nm to over ~2,400 nm. This offers the opportunity to optimize the transmission wavelengths of choice based on where optoelectronic components and amplification technologies present the best performance and achieve the lowest cost per bit, as well as the possibility to provide low-loss transmission at wavelengths that have been so far inaccessible. To quantify the opportunity, more than 70 THz and 105 THz of guidance below 0.1 dB km^{-1} and 0.14 dB km^{-1}, respectively, would be possible for a fibre centred at 1,310 nm. Also, 67 THz and 160 THz below 0.14 dB km^{-1} and 0.2 dB km^{-1}, respectively, would be possible around 1,060 nm, and 100 THz below 0.2 dB km^{-1} seem achievable around 850 nm. The effective exploitation of bandwidths up to ten times wider than in today's telecom C + L would require suitable wideband amplification technologies. To this extent, the tunability of the low-loss transmission wavelength can unlock the possibility to use amplifiers with bandwidth much greater than erbium in the C band (4.5 THz), such as ytterbium at 1,060 nm (13.7 THz)[36], bismuth in the O, E and S bands (21.0 THz)[37], thulium and holmium around 2,000 nm (31.5 THz)[38] or others[39].

Finally, simulations also indicate a potential route to achieve even lower losses than those shown in Fig. 4a. As reported in the literature, LL and SSL in HCFs decrease with increasing core sizes, while µBL has the opposite behaviour[28,29]. By making the fibre stiffer (larger glass outer diameter) and with a thicker coating layer to reduce the µBL contribution, the minimum loss of the fibre can reach lower values at larger core sizes. Figure 4b illustrates our modelling predictions for a fibre operating at 1,550 nm. Starting from the 29.5 µm core diameter of HCF2 (0.07 dB km^{-1} modelled if no asymmetries are present), we see that scaling the core to, say, 40 µm or 50 µm (and by the same ratio also the inter-tube gap sizes and, proportionally, the outer glass diameter and coating thickness), the total loss of the fibre is predicted to decrease

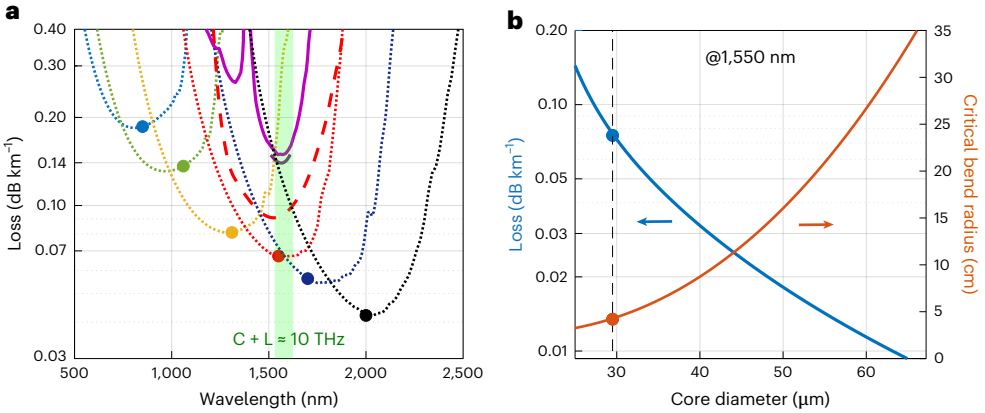

Fig. 4 | Simulated potential performance of further optimized fibres. a, Loss of state-of-the-art PSCFs (pink and purple; Fig. 2), compared with loss of HCF2 (red dashed, gas absorptions omitted) and ideal DNANF with perfect structure (red dotted). The other dotted curves are modelled losses (sum of leakage, surface scattering and microbend loss contributions) of DNANFs with core and tube thicknesses optimized for guidance at 850 nm, 1,060 nm, 1,310 nm, 1,700 nm and 2,000 nm. **b**, Total simulated loss and critical bend radius as a function of core diameter for a 1,550 nm fibre similar to HCF2 with suitably larger core diameter and thicker coating.

to 0.033 dB km^{-1} and 0.018 dB km^{-1}, respectively. Interestingly, even though these fibres would have larger glass tubes than HCF2 with the same membrane thickness, our fluid dynamics model of the fabrication process[40] indicates that their structure is still achievable with standard fabrication methods, with only a modest worsening of their pressure and surface tension-driven dynamics. For example, for a 50 μm core fibre, the pressure buffer that one would have to avoid detrimental mid-draw contact would reduce by only 25% and the sensitivity of a large tube in the final fibre to externally imposed pressure would increase by 2.7 times. Both seem controllable in practice with extra attention and engineering. Clearly, such fibres would be less suitable for high fibre-count cables; they would be stiffer and less bendable, both from a mechanical and an optical point of view. For example, their critical bend radius would increase from 4.2 cm to 8.4 cm and 16 cm, respectively, in the examples above (Fig. 4b). Implementing these changes would necessitate engineering efforts and adjustments to the existing cabling and installation procedures. However, if the performance benefits are validated, these challenges appear manageable.

In conclusion, we have reported what we believe to be one of the most noteworthy improvements in waveguided optical technology for the past 40 years. The pinnacle of 6 years of improvement and optimization, the HCF based on a DNANF design reported here offers a completely new paradigm for transmitting data. In addition to a practically negligible optical nonlinearity[31], the capacity to withstand and transmit three to four orders of magnitude higher powers[41], a 30% reduced latency and a six times reduction in chromatic dispersion compared with standard telecom fibres that is typical of these HCFs, our fibre also presents the lowest loss ever measured in an optical waveguide: 0.091 dB km^{-1} at 1,550 nm and <0.1 dB km^{-1} from 1,481 nm to 1,625 nm (18 THz). Neglecting absorptions from gases in the core and not of fundamental origin, the fibre guides light with <0.2 dB km^{-1} from 1,250 nm to 1,730 nm (66 THz), a 260% improvement over current telecoms fibres (25 THz). Our modelling also indicates that DNANF technology offers in principle the opportunity to tune its lowest-loss transmission window at arbitrary spectral regions in the near infrared (from 700 nm to >2,000 nm). Here, five to ten times wider bandwidth than the current C + L telecoms bands could be achieved, at spectral locations where existing ultra-broad bandwidth amplifiers currently operate, and at lower losses than fundamentally achievable in silica. Finally, we have shown that losses considerably lower than the value reported in this work and towards the 0.01 dB km^{-1} level might be realistically achievable in stiffer fibres with adequately large glass and coated diameters.

In light of the reported results, we are confident that, with advancements in produced volumes, geometrical consistency and reduced presence of absorbing gases in the core, DNANF HCFs will establish themselves as a pivotal waveguiding technology. This innovation has the potential to enable the next technological leap in data communications.

Online content

Any methods, additional references, Nature Portfolio reporting summaries, source data, extended data, supplementary information, acknowledgements, peer review information; details of author contributions and competing interests; and statements of data and code availability are available at https://doi.org/10.1038/s41566-025-01747-5.

References

1. Guarnieri, M. The conquest of the Atlantic. *IEEE Ind. Electron. Mag.* **8**, 53–67 (2014).
2. Buckley, O. Future of transoceanic telephony. *Nature* **150**, 60–62 (1942).
3. Nahin, P. J. *Oliver Heaviside: The Life, Work, and Times of an Electrical Genius of the Victorian Age* (Johns Hopkins Univ. Press, 1987).
4. Kao, K. C. & Hockham, G. A. Dielectric-fibre surface waveguides for optical frequencies. *Proc. Inst. Electr. Eng.* **113**, 1151–1158 (1966).
5. Keck, D. B., Maurer, R. D. & Schultz, P. C. On the ultimate lower limit of attenuation in glass optical waveguides. *Appl. Phys. Lett.* **22**, 307–309 (1973).
6. Agrell, E. et al. Roadmap on optical communications. *J. Opt.* **26**, 093001 (2024).
7. Shannon, C. E. A mathematical theory of communication. *Bell Syst. Tech. J.* **27**, 379–423 (1948).
8. Brewer, S. T., Easton, R. L., Soulier, H. & Taylor, S. A. SG undersea cable system: requirements and performance. *Bell Syst. Tech. J* **57**, 2319–2354 (1978).
9. Kanamori, H. et al. Transmission characteristics and reliability of pure silica-core single-mode fibers. *J. Lightwave Technol.* **4**, 1144–1150 (1986).
10. Sato, S., Kawaguchi, Y., Sakuma, H., Haruna, T. & Hasegawa, T. Record low loss optical fiber with 0.1397 dB/km. In *Proc. Optical Fiber Communication Conference (OFC) 2024* Tu2E.1 (Optica Publishing Group, 2024).
11. Rayleigh, L. XVIII. On the passage of electric waves through tubes, or the vibrations of dielectric cylinders. *Lond. Edinb. Dubl. Philos. Mag. J. Sci.* **43**, 125–132 (1897).

12. Carson, J. R., Mead, S. P. & Schelkunoff, S. A. Hyper-frequency wave guides—mathematical theory. *Bell Syst. Tech. J.* **15**, 310–333 (1936).
13. Barrow, W. L. Transmission of electromagnetic waves in hollow tubes of metal. *Proc. Inst. Radio Eng.* **24**, 1298–1328 (1936).
14. Southworth, G. C. Hyper-frequency wave guides—general considerations and experimental results. *Bell Syst. Tech. J.* **15**, 284–309 (1936).
15. Warters, W. D. WT4 millimeter waveguide system: introduction. *Bell Syst. Tech. J.* **56**, 1873–1897 (1977).
16. Cregan, R. F. et al. Single-mode photonic band gap guidance of light in air. *Science* **285**, 1537–1539 (1999).
17. Russell, P. S. J. Photonic crystal fibers. *Science* **299**, 358–362 (2003).
18. Knight, J., Broeng, J., Birks, T. & Russell, P. Photonic band gap guidance in optical fibers. *Science* **282**, 1476–1478 (1998).
19. Smith, C. M., Venkataraman, N. & Gallagher, M. T. Low-loss hollow-core silica/air photonic bandgap fibre. *Nature* **424**, 657–659 (2003).
20. Benabid, F., Knight, J. C., Antonopoulos, G. & Russell, P. S. J. Stimulated Raman scattering in hydrogen-filled hollow-core photonic crystal fiber. *Science* **298**, 399–402 (2002).
21. Belardi, W. & Knight, J. C. Hollow antiresonant fibers with reduced attenuation. *Opt. Lett.* **39**, 1853–1856 (2014).
22. Poletti, F. Nested antiresonant nodeless hollow core fiber. *Opt. Express* **22**, 23807–23828 (2014).
23. Jasion, G. T. et al. 0.174 dB/km hollow core double nested antiresonant nodeless fiber (DNANF). In *Proc. Optical Fiber Communication Conference (OFC) 2022* Th4C.7 (Optica Publishing Group, 2022).
24. Sakr, H. et al. Hollow core optical fibres with comparable attenuation to silica fibres between 600 and 1100 nm. *Nat. Commun.* **11**, 6030 (2020).
25. Sakr, H. et al. Hollow core NANFs with five nested tubes and record low loss at 850, 1060, 1300 and 1625 nm. In *Proc. Optical Fiber Communication Conference (OFC) 2021* F3A.4 (Optica Publishing Group, 2021).
26. Adamu, A. I. et al. 10.9 km hollow core double nested antiresonant nodeless fiber (DNANF) with 0.33 dB/km loss at 850 nm. In *Proc. Optical Fiber Communication Conference (OFC) 2024* M3J.1 (Optica Publishing Group, 2024).
27. Zhang, X. et al. Low loss nested hollow-core anti-resonant fiber at 2 μm spectral range. *Opt. Lett.* **47**, 589–592 (2022).
28. Numkam Fokoua, E. R., Abokhamis Mousavi, S. M., Jasion, G., Richardson, D. & Poletti, F. Loss in hollow-core optical fibers: mechanisms, scaling rules, and limits. *Adv. Opt. Photon.* **15**, 1–85 (2023).
29. Chen, Y. et al. Hollow core DNANF optical fiber with <0.11 dB/km loss. In *Proc. Optical Fiber Communication Conference (OFC) 2024* Th4A.8 (Optica Publishing Group, 2024).
30. Downie, J. D. et al. Quasi-single-mode fiber transmission for optical communications. *IEEE J. Sel. Top. Quantum Electron.* **23**, 31–42 (2017).
31. Poggiolini, P. & Poletti, F. Opportunities and challenges for long-distance transmission in hollow-core fibres. *J. Lightwave Technol.* **40**, 1605–1616 (2022).
32. Gao, S. et al. Fourfold truncated double-nested antiresonant hollow-core fiber with ultralow loss and ultrahigh mode purity. *Optica* **12**, 56–61 (2025).
33. Gordon, I. E. et al. The HITRAN2020 molecular spectroscopic database. *J. Quant. Spectrosc. Radiat. Transf.* **277**, 107949 (2022).
34. Nagayama, K., Kakui, M., Matsui, M., Saitoh, T. & Chigusa, Y. Ultra-low-loss (0.1484 dB/km) pure silica core fibre and extension of transmission distance. *Electron. Lett.* **38**, 1168–1169 (2002).
35. Hong, Y. et al. Low-latency WDM intensity-modulation and direct-detection transmission over >100 km distances in a hollow core fiber. *Laser Photon. Rev.* **15**, 2100102 (2021).
36. Huang, X., Liang, S., Xu, L., Richardson, D. J. & Jung, Y. Wideband (13.7 THz) gain-flattened Yb-doped fiber amplifier for telecommunication applications. *IEEE Photon. Technol. Lett.* **36**, 791–794 (2024).
37. Zhai, Z. & Sahu, J. K. High-gain ultra-wideband bismuth-doped fiber amplifier operating in the O+E+S band. *Opt. Lett.* **49**, 3308–3311 (2024).
38. Tench, R. E. Design of a novel 31.5 THz bandwidth hybrid TDFA-HDFA at 2000 nm and its applications in unregenerated DWDM lightwave transmission systems. *J. Opt. Photon. Res.* https://doi.org/10.47852/BONVIEWJOPR42024305 (2024).
39. Renaudier, J. et al. Devices and fibers for ultrawideband optical communications. *Proc. IEEE* **110**, 1742–1759 (2022).
40. Jasion, G. T. et al. Fabrication of tubular anti-resonant hollow core fibers: modelling, draw dynamics and process optimization. *Opt. Express* **27**, 20567–20582 (2019).
41. Mulvad, H. C. H. et al. Kilowatt-average-power single-mode laser light transmission over kilometre-scale hollow-core fibre. *Nat. Photon.* **16**, 448–453 (2022).

Methods

Modelling loss validation

To calibrate and validate our loss models, we acquired SEM images of the end faces of 15 fabricated DNANFs, each with 5 sets of nested tubes like the one in Fig. 1a, but with geometrical parameters (core diameter, tube sizes and membrane thicknesses) varying by up to 5–20%. We then reconstructed the contours of their geometrical structure using the procedure above and performed finite element mode-solving calculations on the resulting permittivity profiles. This solution yields the LL of each mode from the imaginary part of the eigenvalue associated with it. Knowledge of the eigenvalue or mode propagation constants across wavelengths is also used to calculate both the group delay (latency) and chromatic dispersion (such as shown in Fig. 3b) from the first and second derivatives with respect to optical frequency, respectively. From the mode-field distributions, we computed the normalized field intensity near the glass interfaces F as well as the mode spot area w_0 that are used in SSL and μBL models[41]. Here two unknown parameters are used to empirically characterize the roughness of the glass-air surfaces, ultimately caused by frozen-in surface capillary waves, while two more are used to represent the power spectral density of the external perturbations that lead to microbending. To fit these four parameters, we measured the loss of the 15 different DNANFs. We then extracted their geometry and fitted their calculated total loss, that is, the sum of LL, SSL and μBL, to the measured loss curves. We hence obtained a unique set of values for these four non-directly measurable coefficients that ensured the best agreement between measured and total simulated loss for all fibres simultaneously. One example of the comparison between simulation and measurement is shown in Fig. 1a.

Fibre fabrication

The fibre fabrication involved a two-stage stack, fuse and draw technique, where cladding capillaries surrounding a central air core, composed of five outer silica tubes with two sets of five nested middle and inner tubes, were stacked and fused within a jacket tube and then drawn into intermediate size canes. These canes were subsequently reduced to fibre dimensions using a cane-in-tube drawing process. During the fibre drawing, the core region and the three regions between and inside cladding tubes were pressurized independently. The thicknesses of the three sets of five cylindrical silica membranes surrounding the core were engineered to ~500 nm to centre the first antiresonant window to around 1,550 nm.

Distributed loss measurements via optical time-domain reflectometry

The fibre length and the distributed loss of the fibre were measured using a bi-directional OTDR method. One advantage of performing bi-directional measurements is that through simple theory[42], one can separate the longitudinal loss dependence from any local transient change in scattering caused by gas pressure gradients along the fibre[43]. These transients are typically present near both ends of an HCF, owing to the ingress of air at atmospheric pressure. In our measurement, the OTDR (Viavi E41DWDMC) was amplified to compensate for the DNANF's 30 dB lower backscattering than in glass-core fibres[44], and coupled into the fibre under test through a spliced mode-field adaptor. Thanks to the low optical nonlinearity of DNANF, we were able to boost the pulse energy launched into the fibre using an erbium-doped fibre amplifier, thereby increasing the dynamic range of the measurement. The measurements were performed with a time resolution of 10–30 ns, corresponding to a spatial resolution of 1.5–4.5 m. Measurements at 1,310 nm and at 1,550 nm shown in Fig. 2b clearly show uniform loss across the full fibre length.

Broadband optical attenuation measurement via cutback

The optical attenuation of the fibres was also measured using a cutback technique. The full length of the fibre, measuring 15 km, was spooled on a bobbin of 1 m circumference with a short length of 20 m deployed loosely on the optical bench. Two different sets of equipment (A and B) were used. Set A involved spectral measurements using an intensity-stabilized tungsten white light source (Bentham WLS100) as a broadband source and an OSA (Yokogawa AQ-6315A, wavelength range 400–1,750 nm, but rather noisy after 1,650 nm). Set B consisted of a white light source, a monochromator and a photodetector, integrated within a commercial loss-measurement device. With set A, the DNANF input end was spliced to a mode-field-adapted solid core patch cord and kept unaltered. Transmission traces from three different cleaves of the DNANF output end were then recorded in the OSA for the full fibre length, then the fibre was cut to 20 m and three more traces corresponding to three different cleaves were acquired. The average transmission for each length was used to calculate the spectral loss trace. We repeated this cutback procedure three times. With set B, we also applied a cutback procedure to acquire one additional loss trace. Here the launch into the DNANF under test occurred through a free-space mode-field-adapted beam. As this method is virtually independent on the quality of the cleaves, there was no need to acquire multiple cleaves. The four cutbacks returned similar traces, despite the use of different launch and measurement set-ups.

Mean loss, confidence level and loss measurement at long wavelengths

From the four independent cutback measurements, we calculated the spectral dependence of the mean loss (dark blue curve in Fig. 2c) and its standard deviation σ. The confidence level (CL) around the mean value, shown by the green shaded area around the blue line, was calculated as $\mathrm{CL} = z^*\sigma/\sqrt{n}$, with $z^* = 1.96$ for a confidence level of 95% and $n = 4$. We also performed a fifth 20 m cutback using a white light source and a long wavelength OSA (Yokogawa AQ-6375E, wavelength range 1,200–2,400 nm) to acquire the full spectral loss of the fibre, even beyond the wavelength of 1,650 nm where the previous measurement becomes too noisy. This additional measurement is shown by the light blue trace in Fig. 2c. The whole curve has been translated vertically so that it matched the loss of the more accurate dark blue curve at 1,650 nm.

IMI measurement

IMI is an impairment in the transmitted signal caused by beating between the signal in the fundamental mode and weak replicas caused by multiple scattering events into the slower higher-order modes and back into the fundamental mode. The incoherent interference between the signal and its weak delayed replica leads to noise, which we measured here using a swept wavelength scanning method. We used a tunable laser source with a wavelength resolution of 0.2 picometres and a fast power meter. IMI is calculated using the following formula[45]:

$$\alpha^2 = \frac{1}{2}\left(\frac{\sigma}{P_{\mathrm{av}}}\right)^2,$$

where P_{av} is the average power of the measurement across a 2 nm window centred at 1,555 nm, and σ is the standard deviation around it.

Simulation of wavelength scaling

To investigate the loss and bandwidth that could be potentially achievable in DNANFs similar to HCF2 at other wavelengths, we exploit the principle that in antiresonant HCFs the membrane thickness can be modified for operating at a different wavelength λ by ensuring that the normalized frequency $f = \frac{2t\sqrt{n^2-1}}{\lambda}$ remains constant. Here we calculated the thicknesses required for operation at 850 nm, 1,060 nm, 1,310 nm, 1,700 nm and 2,000 nm. In this study, we used an idealized version of HCF2 (with no asymmetries) and scaled all its membrane thicknesses by the same factor. Next, for each fibre, we scaled the core size. We assumed that (1) our calibrated loss models retain their accuracy across

the 700–2,400 nm wavelength range, and (2) the fibres maintained the same outer diameter as HCF2. We then used the values for LL, SSL and μBL obtained for 1,550 nm and their scaling rules with core size[29] to identify the core diameter that minimized the overall loss at each central wavelength of interest. We then repeated the mode-solving and loss calculations for each optimized fibre. It is important to note that lower losses than those shown in Fig. 4a may be potentially achievable, since the simulated structures reported here are based on the structure of HCF2, which reflect our current fabrication processes, rather than the absolute best DNANFs possible.

Performance extrapolation in fibres with larger core sizes

Next, we investigated whether a further reduction in attenuation may be possible by enlarging the fibre core size. For this study, we only considered the 1,550 nm case and started by the ideal HCF2, where SSL is the dominant loss mechanism and LL and μBL only play a small contribution. LL and SSL are known to scale inversely proportionally with the fibre's core diameter. In contrast, μBL increases steeply with the mode spot area, which is directly proportional to the core diameter[41]. It is however well known that μBL can be reduced by improving how the fibre packaging absorbs the external perturbations. For example, this can be achieved by increasing the diameter of the glass to make the fibre stiffer and more resistant to external lateral loads, or by use of coating materials with different mechanical properties, for example, lower Young's modulus. Here we considered fibres with the same membrane thickness as HCF2 but with increasingly larger core size (and proportionally larger tube diameters and wider inter-tube gaps). As the core enlarged, we increased the total fibre diameter such that the μBL contribution would remain only a small fraction of the total loss. Since LL decreases more rapidly than SSL with increasing core diameter, this study essentially obtained the SSL-limited loss of the fibre. For all fibres, we assumed a coating with the same mechanical properties as HCF2 but with a thickness proportional to the core size. The result of mode-solving simulations and loss calculations at 1,550 nm for fibres with core diameter from 29 μm to 65 μm is shown in Fig. 4b. One downside of the overall reduction in loss is that as the core diameters increase, the fibres become less bendable. To quantify this, we also calculated the bend loss for each fibre as a function of bend radius. To simulate bend loss, we used the well-known transformation optics approach, where the distribution of the refractive index n in the cross section is mapped as $n(x,y) \rightarrow n(x,y)\,e^{\frac{x}{R_b}}$, and R_b is the bend radius. For each fibre, we then determined and plotted the critical bend radius, defined as the radius causing the loss to double from that of the straight fibre.

Data availability

The data included in this paper can be accessed at https://doi.org/10.5258/SOTON/D3594.

References

42. Di Vita, P. Mode power distribution in optical fibres with fluctuation in physical parameters and application to backscattering signal analysis. *Electron. Lett.* **17**, 874–876 (1981).
43. Wei, X., Shi, B., Richardson, D. J., Poletti, F. & Slavik, R. Distributed characterization of low-loss hollow core fibers using EDFA-assisted low-cost OTDR instrument. In *Proc. Optical Fiber Communication Conference (OFC) 2023* W1C.4 (Optica Publishing Group, 2023).
44. Numkam Fokoua, E., Michaud-Belleau, V., Genest, J., Slavík, R. & Poletti, F. Theoretical analysis of backscattering in hollow-core antiresonant fibers. *APL Photon.* **6**, 96106 (2021).
45. Ramachandran, S., Nicholson, J. W., Ghalmi, S. & Yan, M. F. Measurement of multipath interference in the coherent crosstalk regime. *IEEE Photon. Technol. Lett.* **15**, 1171–1173 (2003).

Acknowledgements

This work was partly funded by the ESPRC Prosperity Partnership Programme FASTNET, EP/X025276/1 (M.P., E.N.F., G.J. and F.P. as investigators). We would like to gratefully acknowledge S. Bakhtiari Gorajoobi, R. Slavík, X. Wei, M. Alonso, K. Wisniowski and L. Budd for substantial contributions to improving techniques and instruments tailored to the characterization of HCFs; A. Boyland, L. Hooper, G. Babiarz, T. Varghese, D. Suslov and M. Fatobene Ando for contributions to developing and improving manufacturing processes related to HCF production; and J. Gaudette, D. Richardson, A. Harker, A. Appleyard, S. Doran, G. Amouzad Mahdiraji and J. Rzegocki for constructive discussions related to HCF technology that have contributed indirectly to the result reported in this work.

Author contributions

M.P. and Y.C. led the fabrication activities and the fibre process development. E.N.F. led the modelling activities for the fabricated and the future potential fibres. H.S. led the fibre characterization. A.I.A., R.H. and D.W. contributed to manufacturing processes and fabricated the fibres. R.F.A. developed a model to extract the HCF cross-sectional parameters. A.P. carried out modelling for HCF structural optimization. S.R.S. contributed to improving manufacturing and characterization processes. G.J. developed and run fluid dynamics draw models. F.P. instigated the study, provided the overall scientific leadership and wrote the paper.

Competing interests

Microsoft currently uses hollow core fibres of the type discussed in this paper within their own private network. Aspects of the technology are protected by patents owned by the University of Southampton or by Microsoft, including patent WO2015/185761 that protects the design discussed in this work.

Additional information

Supplementary information The online version contains supplementary material available at https://doi.org/10.1038/s41566-025-01747-5.

Correspondence and requests for materials should be addressed to Francesco Poletti.

Peer review information *Nature Photonics* thanks Jonathan Knight and the other, anonymous, reviewer(s) for their contribution to the peer review of this work.